J Mater Sci (2011) 46:2431–2436
DOI 10.1007/s10853-010-5089-9

Preparation, thermostability, and spectroscopic properties of Rhodamine 6G intercalated titanoniobate nanocomposite

**Juanjuan Ma · Xinxin Ban · Jingfei Li ·
Heng Jiang · Tianlin Zhang · Lin Liu ·
Xingyou Xu · Zhiwei Tong**

Received: 3 July 2010 / Accepted: 16 November 2010 / Published online: 30 November 2010

Abstract Rhodamine 6G (R6G), a well-known fluorescent dye, has been intercalated into layered potassium titanoniobate ($KTiNbO_5$) through a guest–guest exchange method by using propylammonium titanoniobate ($PrNH_3{}^+$-$TiNbO_5$) as a precursor. The synthesis process, the structure and morphology characterizations for lamellar nanocomposite have been investigated by means of XRD, FTIR, and SEM. The thermostability of $R6G^+$-$TiNbO_5$ nanocomposite is discussed on the basis of thermogravimetric and calorimetric techniques. Absorption and fluorescence techniques are applied to study the photoresponse of R6G in hybrid film. The results indicate that $R6G^+$ cations in thin film are highly fluorescent even at a high dye concentration, which may be due to the formation of J-dimers within the confined galleries.

Introduction

Nanocomposites derived from photoactive molecules associated with layered inorganic solids have attracted considerable attention for the design of new optical, photonic, and photoelectronic devices with potential applications as tunable solid-state lasers, optical switches, double-frequency crystals, solar cells, etc. [1–3]. The guest molecules are able to exhibit unique properties because the guest species interact with both the host layers sandwiching them and other intercalated molecules arranged in the interlayer spaces. Among the many inorganic host materials, two-dimensional semiconducting crystallites of titanium oxide and niobium oxide are interesting hosts. Compared with other layered compounds, these nanosheets possess a high negative charge density, a high anisotropy, and an ultrathin thickness, which allow the intercalation compounds to show peculiar photofunctions, e.g., photoinduced electron transfer and photosensitization. Following these ideas, in recent decade interest has focused on the photofunctions of niobates and titanates intercalated with methylene blue [4], methyl viologen [5], porphyrin [6, 7], and ruthenium complex [8, 9].

On the other hand, Rhodamine 6G (R6G) is chosen as guest molecule because it is a cationic xanthene dye with a high capacity to absorb and to emit light in the visible region. However, R6G shows a strong tendency to form aggregates when dissolved in concentrated solution, which may drastically modify the optical properties of the dye [10]. For example, at 10^{-4} M the R6G aqueous solution does not show any lasing capability. In the past few decades, hybrid materials were prepared by introducing R6G molecules into solid matrixes of inorganic (clays [11–13], silica glass [14, 15], molecular sieve [16], and transition metal oxides [17–19]) and polymeric (PMMA [20], SSEBS tri-block copolymer [21]) nature. And it has been well documented that the environmental factors (polarity, charge, etc.) could have an important influence on the spectroscopic and optical properties of aggregated dyes.

J. Ma · X. Xu
Key Laboratory of Soft Chemistry and Functional Materials,
Ministry of Education, Nanjing University of Science
and Technology, Nanjing 210094, China

J. Ma · X. Ban · J. Li · H. Jiang · T. Zhang · L. Liu ·
Z. Tong (✉)
Department of Chemical Engineering, Huaihai Institute
of Technology, Lianyungang 222005, China
e-mail: zhiweitong575@hotmail.com

X. Xu
School of Life Science and Chemical Engineering,
Huaiyin Institute of Technology, Huaian 223003, China

Z. Tong
SORST, Japan Science and Technology (JST),
Kawaguchi, Japan

For instance, enhanced fluorescence of R6G was observed in the channels of MCM-41 mesophase [16].

Recently, Nakato et al. [22, 23] have reported the synthesis of the intercalation compound of hexaniobate ($K_4Nb_6O_{17}$) with R6G dye. These reports prompted us to examine a preparation of novel R6G intercalated potassium titanoniobate ($KTiNbO_5$) (Fig. 1) nanocomposite by a guest–guest exchange process. X-ray diffraction (XRD) and infrared (IR) spectra were measured to confirm the incorporation of cationic dyes into the interlayer space of titanoniobate. The morphology of the compound was checked by scanning electron microscopy (SEM). In addition, DSC and TG analysis measurements were used to analyze the thermostability of the new hybrid. Finally, absorption and fluorescence spectroscopic data have also been obtained, from which the aggregation state of dye molecules in constrained and rigid nanostructured environment can be evaluated.

Experimental

Materials

A layered compound $KTiNbO_5$ was synthesized by heating homogeneously mixed powders of K_2CO_3, TiO_2, and Nb_2O_5 (anatase, high-purity chemicals) in molar ratios of 1:2:1 at 1,150 °C, according to the procedure described in the literature [7]. Commercially available chloride salt of R6G (Sigma) and *n*-propylamine (Sinopharm Chemical Reagent CO., Ltd) were used without further purification.

Intercalation of R6G into layered titanoniobates

1.0 g of $KTiNbO_5$ powder sample was treated three times with 1 M HCl for 24 h at room temperature. The titanoniobic acid formed was washed with deionized water until free of Cl^-, and then dried in air. 0.5 g of titanoniobic acid was sealed in an ampule with 15 mL of a 50% *n*-propylamine aqueous solution and allowed to stand for 2 weeks at room temperature. The precipitate powder was washed with alcohol and dried in air. The obtained white powder of propylammonium titanoniobate ($PrNH_3^+$-$TiNbO_5$) was again sealed with 0.05 M aqueous solution of $R6G^+$ at 60 °C for 3 weeks. The $R6G^+$ solution was adjusted to a pH of 6 with *n*-propylamine. The reaction was carried out in the dark in order to avoid photodegradation of R6G. The resultant solution was centrifuged and washed with methanol and water thoroughly to obtain a red powder of $R6G^+$-$TiNbO_5$ nanocomposite. The intercalation compound was dispersed in deionized water with sonication and cast on quartz substrates, so that optically transparent $PrNH_3^+$-$TiNbO_5$ and $R6G^+$-$TiNbO_5$ hybrid thin films were obtained and used for further structural characterization.

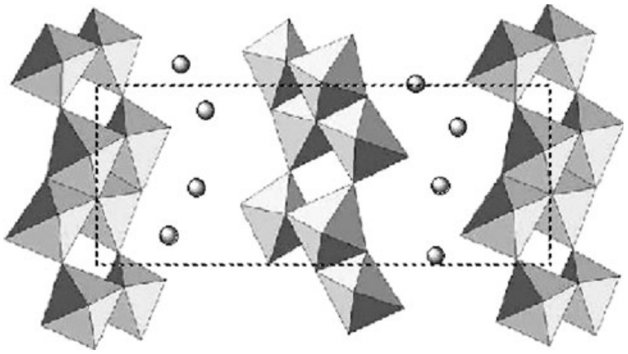

Fig. 1 Structure of $KTiNbO_5$. *Squares* represent the TiO_6 (and NbO_6) octahedra, and *circles* indicate the exchangeable cation K^+ in the interlayer

Characterization

XRD profiles were obtained with a RINT 2000 diffractometer (Rigaku), using Cu K_α radiation ($\lambda = 0.154$ nm) with 2θ going from 2.5° to 40° in 1.0° steps. SEM images were taken with a JSM-5600 apparatus (JEOL) operating at 20 kV for the Au-coated samples. IR spectra were recorded on a Shimadzu FTIR-8400S spectrometer in solid KBr pellets. The composition of the $R6G^+$-$TiNbO_5$ hybrid was performed using a Perkin Elmer 2400-CHN elemental analyzer. DSC and TG analysis measurements were carried out with a Netzsch Sta 409 PC/PG apparatus at a heating rate of 20 °C min^{-1} under dry nitrogen. Visible absorption spectra were recorded on a Varian spectrometer (model CARY 50). The emission spectra were measured on a spectrofluorometer (model FL3-TCSPC, Horiba Jobin-Yvon).

Results and discussion

Incorporation of R6G molecules into layered titanoniobate

The incorporation of bulky ions into the interlayer spaces of titanoniobates is difficult owing to the high charge densities of $TiNbO_5^-$ layers. Herein, we have employed a guest–guest exchange method and successfully incorporated $R6G^+$ cations into the layered titanoniobate. The XRD pattern of $KTiNbO_5$ (Fig. 2a) indicates that this compound is obtained as a single phase. The protonation of $KTiNbO_5$ causes the basal spacing to be shortened to 0.85 nm (Fig. 2b). The propylammonium ions intercalated compound with 1.57 nm of the d_{002} (Fig. 2c) is subsequently treated with $R6G^+$ to produce a $R6G^+$-$TiNbO_5$ hybrid, resulting in an increase of the d_{002} value to 2.26 nm

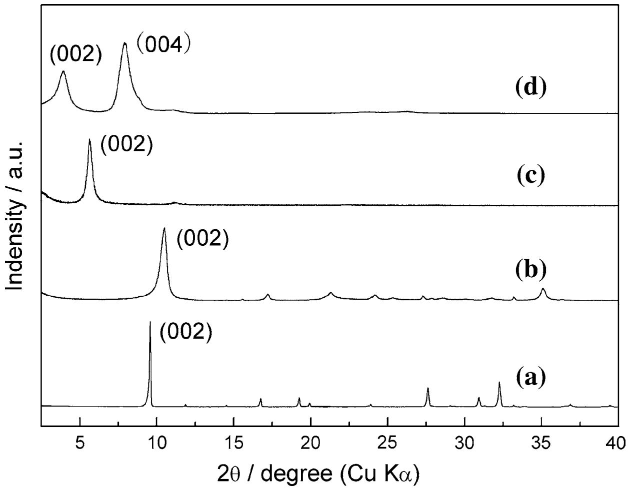

Fig. 2 XRD patterns of **a** $KTiNbO_5$, **b** $HTiNbO_5$, **c** $PrNH_3^+$-$TiNbO_5$, and **d** $R6G^+$-$TiNbO_5$

Table 1 XRD spectrum data

Compound	d_{002} (nm)	Δd^a (nm)
$KTiNbO_5$	0.92	0.24
$HTiNbO_5$	0.85	0.17
$PrNH_3^+$-$TiNbO_5$	1.57	0.89
$R6G^+$-$TiNbO_5$	2.26	1.58

[a] Δ*d* is gallery height

(Fig. 2d). The basal spacings of these products are listed in Table 1. By subtracting the thickness of $TiNbO_5^-$ slab (0.68 nm) [24], the net interlayer height of $R6G^+$-$TiNbO_5$ can be calculated as 1.58 nm. Considering the R6G molecular dimension (1.38 × 1.15 × 0.90 nm) [25], it is postulated here that $R6G^+$ forms monolayer coverage with its long molecular axis being oriented perpendicular with respect to titanoniobate nanosheets (Fig. 3).

Figure 4 shows a sequence of SEM of $KTiNbO_5$ as starting material (a), after acid treatment (b), after preintercalation in the presence of *n*-propylamine ($PrNH_3^+$-$TiNbO_5$) (c), and after ion exchange with $R6G^+$ ($R6G^+$-$TiNbO_5$) (d). From Fig. 4a, we can see that the original $KTiNbO_5$ consists of plate-like texture reflecting its layered structure. The texture of the particles remains almost unchanged after the acid treatment process (Fig. 4b). Exfoliation of titanoniobate nanosheets can be observed in the SEM image of $PrNH_3^+$-$TiNbO_5$ (Fig. 4c). And the structure of the intermediate is basically retained in the resultant intercalation compound $R6G^+$-$TiNbO_5$ (Fig. 4d).

The intercalation of $R6G^+$ ions is also supported by IR spectroscopic analysis. Many characteristic absorption peaks of $R6G^+$ can be observed in the IR spectrum of $R6G^+$-$TiNbO_5$ hybrid (Fig. 5b) [22]. The 1320 cm^{-1} peak is assigned to the aryl C–N stretching and the peaks at 1611, 1529, and 1501 cm^{-1} are associated with in-plane vibration of the xanthene ring. The absorption peak at 1721 cm^{-1} is attributed to C=O stretching vibration in the carbonyl–phenyl group. The bands in the range of 400–1000 cm^{-1} arise from the Nb–O and Ti–O stretching vibration of the layered host [4]. On the basis of elemental analysis (C, H, and N distribution of 26.36, 3.42, and 2.21%, respectively), the calculated formula for $R6G^+$-$TiNbO_5$ hybrid is $(R6G^+)_{0.3}H_{0.7}TiNbO_5 \cdot 1.5H_2O$. The experimental C/N molar ratio is 13.92, which is in agreement with the expected value of 14.0. These results indicate that propylammonium ions are completely removed from the $R6G^+$-$TiNbO_5$ hybrid during the guest–guest exchange procedure. And the dye loading in the hybrid can be estimated as 34.8 wt%.

Thermal analysis

The thermal stability of the R6G molecules in solid host material has been investigated by thermogravimetry and calorimetric techniques in an inert N_2 atmosphere. Figure 6 shows the TGA and DSC thermograms of pure R6G and R6G-$TiNbO_5$ hybrid. Both TGA curves exhibit a several-step weight loss process. And the weight loss of organic matter in the $R6G^+$-$TiNbO_5$ hybrid is slower and is extended to higher temperatures (at around 600 °C) than the pure dye (sharp weight loss in the 270–540 °C range). The DSC of R6G displays a small endothermic effect at about 266 °C due to incipient melting, followed by two exothermic peaks related to sample decomposition [14]. The first and sharp one at ~320 °C is attributed to the decomposition of $-COOCH_2CH_3$ group. The second and broader one at ~500 °C is due to the decomposition of the skeleton of the molecule. On the other hand, the DSC curve for $R6G^+$-$TiNbO_5$ hybrid shows a endothermic peak at ~106 °C, which can be ascribed to the removal of water molecules from the gallery space. Similar to the pure dye molecule, the following two overlapping exothermic peaks corresponds to the decomposition of R6G molecules in the hybrid. However, in this case, the dye degradation takes place at higher temperatures with the first exothermic effect at ~384 °C and the second one at ~530 °C. This result suggests that the intercalation of dye molecules in solid inorganic host material enhances thermostability of the dye.

Spectroscopic properties of $R6G^+$-$TiNbO_5$ hybrid

Comparison of the visible absorption spectra of a $R6G^+$ intercalated titanoniobate film and a $R6G^+$ aqueous solution is shown in Fig. 7. In $R6G^+$ aqueous solution, the main band at 526 nm and shoulder at about 500 nm are

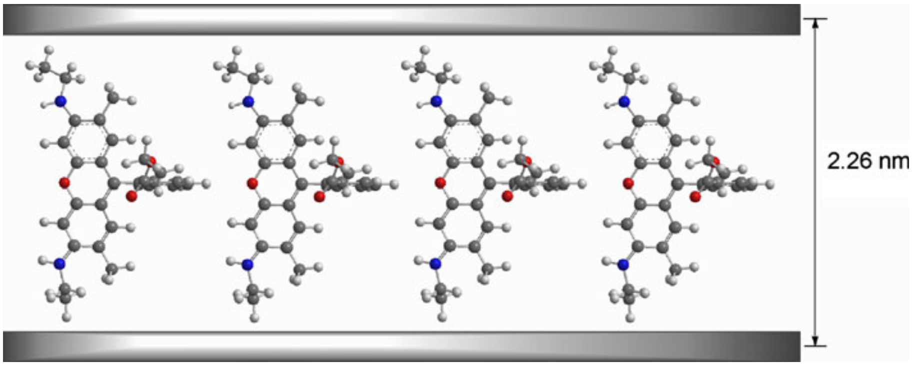

Fig. 3 Intercalation model of R6G$^+$-TiNbO$_5$

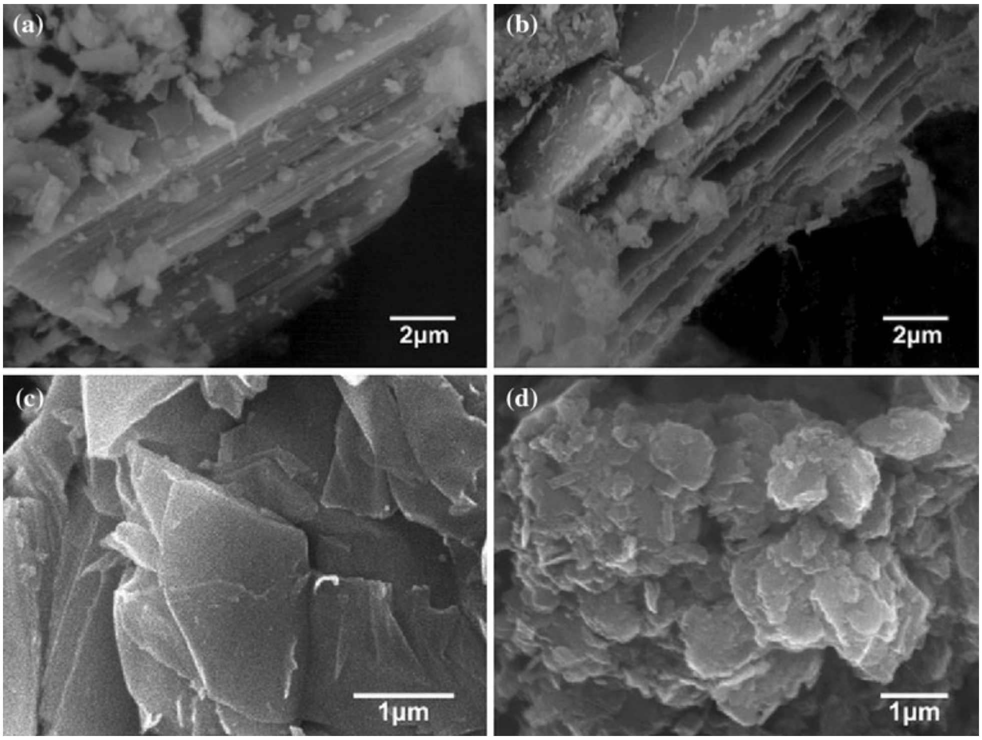

Fig. 4 SEM images of **a** KTiNbO$_5$, **b** HTiNbO$_5$, **c** PrNH$_3$$^+$-TiNbO$_5$, and **d** R6G$^+$-TiNbO$_5$

observed. The former is associated with the absorption by monomeric dye and the latter is due to the formation of H-dimer (placed at higher energies than the monomer absorption band). When R6G$^+$ cations are inserted into the titanoniobate layers, the main band is shifted to longer wavelength ($\Delta\lambda = 14$ nm). Similar phenomena in the visible absorption spectra of R6G have also been observed in other solid matrices. For example, Grauer et al. [26] studied the adsorption and intercalation of R6G$^+$ in montmorillonite and Laponite and found red shifts of 20 and 13 nm, respectively. Conversely, Nakato et al. [22] reported shorter wavelength shift when they studied the spectroscopic behavior of R6G$^+$ intercalated layered niobate. The red shift of the main peak has been attributed to the formation of the J-dimer (placed at lower energies than the monomer absorption band), which is not present in the bulk aqueous solution except at very high concentrations. In general, the matrix polarity has an important influence on the aggregation state of dye molecules in confined spaces and less polar media favors the formation of the J-dimer. In our case, the interlayer spaces are more hydrophobic as compared to the aqueous solution system. In the spectrum of hybrid film, the shoulder at about 500 nm can also be observed, indicating the presence of H-dimer. As the H-excites states of aggregates are not fluorescent, the absorption technique is a more appropriate method to spectroscopically characterize the dimerization process of dyes. This coexistence of H-dimers and J-dimers of rhodamines in different surfaces and interfaces has been also proposed by several authors [27, 28].

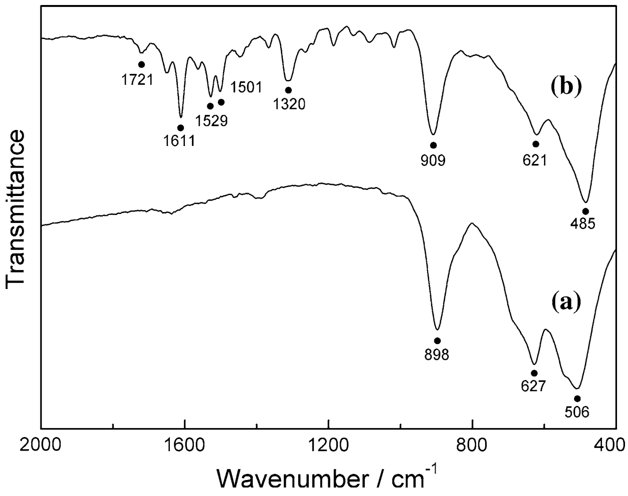

Fig. 5 IR spectra of **a** $KTiNbO_5$ and **b** $R6G^+$-$TiNbO_5$

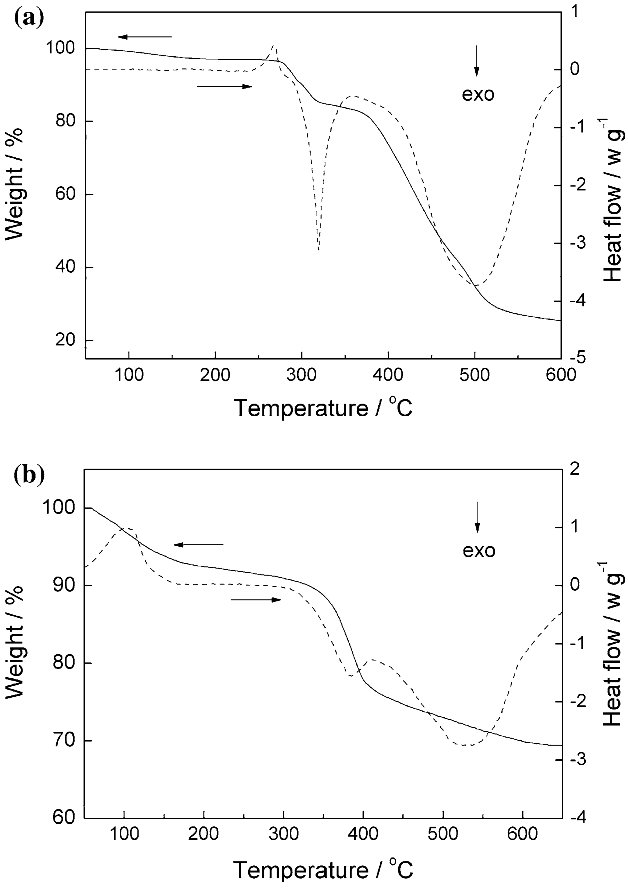

Fig. 6 TGA (*solid line*) and DSC curves (*dashed line*) of **a** pure R6G and **b** $R6G^+$-$TiNbO_5$

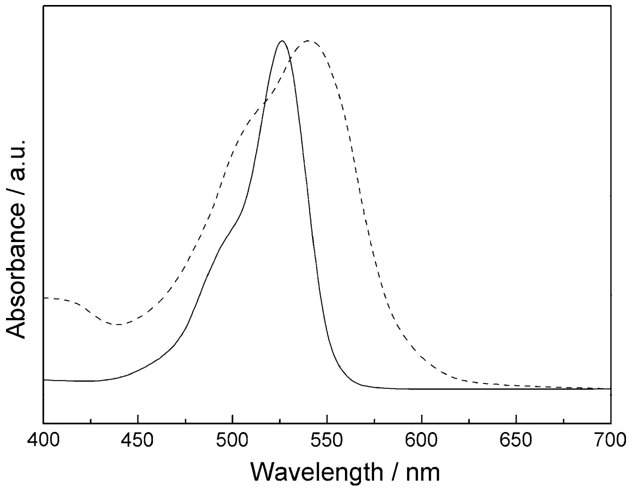

Fig. 7 Normalized absorption spectra of 10^{-5} M R6G aqueous solution (*solid line*) and the film deposited from $R6G^+$-$TiNbO_5$ hybrid (*dashed line*)

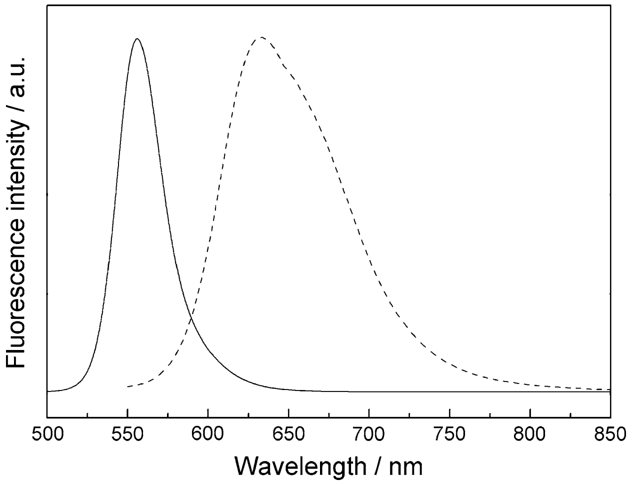

Fig. 8 Normalized emission spectra of 10^{-5} M R6G aqueous solution (*solid line*) and the film deposited from $R6G^+$-$TiNbO_5$ hybrid (*dashed line*), obtained by excitation at $\lambda = 482$ nm

Fluorescence spectra for solution phase and nanocomposite system are acquired (see Fig. 8). We are delightly to find that $R6G^+$ cations in thin film are highly fluorescent with efficiencies even at a high concentration. This is quite different from the photophysical behavior of dye in aqueous solution, where undesirable concentration quenching caused by the formation of H-dimer is often observed. When $R6G^+$ cations are intercalated in the titanoniobate layers, the emission maximum is red shifted from 555 to 633 nm, suggesting the formation of fluorescent J-dimer species [29]. As proposed above, the matrix polarity can also be used to explain the observed red shift in the luminescence. Besides, it can be seen that the emission band of $R6G^+$ intercalated titanoniobate film has been remarkably broadened as compared to that of dye in water. This implies that the nearest-neighbor structure around the dye is not so simple as the cluster structure of solvation in solution. In fact, intramolecular charge transfer caused by host–guest interaction has been reported for intercalation compounds of semiconducting oxides with dyes [30]. Similar interactions may occur in present system.

Conclusions

This is the first successful example of a R6G/$KTiNbO_5$ intercalation compound. The insertion of $R6G^+$ was confirmed by the change in the color (from white to red) and the expansion of the basal spacing (from 0.92 to 2.26 nm). The intercalated $R6G^+$ cations form monolayer coverage with long molecular axis being oriented perpendicular with respect to titanoniobate nanosheets. The incorporation of cationic dyes in the bidimensional nanostructure produces a red shift in the absorption band of the dye. The coexistence of H-dimers and J-dimers of $R6G^+$ in interlayer space of titanoniobate is proposed. The solid matrix offers a larger thermal stability and allows emission of fluorescence even at a high dye concentration. $R6G^+$-$TiNbO_5$ hybrid possesses a good quality in optical properties and is an excellent host–guest solid-state system with possible photofunctional applications.

Acknowledgement This work was supported by National Natural Science Foundation of China (Grant No. 50873042) and the Scientific Research Program of the HuaiHai Institute of Technology (Z2009021).

References

1. Schulz-Ekloff G, Wohrle D, van Duffel B, Schoonheydt RA (2002) Micropor Mesopor Mater 51:91
2. Arbeloa FL, Martinez VM, Arbeloa T, Arbeloa IL (2007) J Photochem Photobiol C 8:85
3. Unal U, Matsumoto Y, Tamoto N, Koinuma M, Machida M, Izawa K (2006) J Solid State Chem 179:33
4. Zhang XB, Liu C, Liu L, Zhang DE, Zhang TL, Xu XY, Tong ZW (2010) J Mater Sci 45:1604. doi:10.1007/s10853-009-4134-z
5. Nakato T, Edakubo H, Shimomura T (2009) Micropor Mesopor Mater 123:280
6. Bizeto MA, de Faria DLA, Constantino VRL (2002) J Mater Sci 37:265. doi:10.1023/A:1013687825874
7. Tong ZW, Shichi T, Oshika K, Takagi K (2002) Chem Lett 31:876
8. Tong ZW, Takagi S, Tachibana H, Takagi K, Inoue H (2005) Chem Lett 34:608
9. Yao K, Nishimura S, Imai Y, Wang H, Ma TL, Abe E, Tateyama H, Yamagishi A (2003) Langmuir 19:321
10. Malfatti L, Kidchob T, Aiello D, Aiello R, Testa F, Innocenzi P (2008) J Phys Chem C 112:16225
11. Martinez VM, Arbeloa FU, Prieto JB, Lopez TA, Arbeloa IL (2004) Langmuir 20:5709
12. Iyi N, Sasai R, Fujita T, Deguchi T, Sota T, Arbeloa FL, Kitamura K (2002) Appl Clay Sci 22:125
13. Fujita T, Iyi N, Kosugi T, Ando A, Deguchi T, Sota T (1997) Clay Clay Miner 45:77
14. Grandi S, Tomasi C, Mustarelli P, Clemente F, Carbonaro CM (2007) J Sol-Gel Sci Technol 41:57
15. Carbonaro CM, Anedda A, Grandi S, Magistris A (2006) J Phys Chem B 110:12932
16. Yao YF, Zhang MS, Yang YS, Su Q, Zhang HJ (2002) Chin Chem Lett 13:464
17. Ara K, Tagaya H, Ogata T, Matsushita K, Kadokawa J, Karasu M, Chiba K (1996) Mater Res Bull 31:283
18. Matsuo Y, Yamada N, Fukutsuka T, Sugie Y (2006) Mol Cryst Liq Cryst 452:137
19. Hamad S, Sanchez-Valencia JR, Barranco A, Mejias JA, Gonzalez-Elipe AR (2009) Mol Simul 35:1140
20. Perez-Bueno JJ, Vasquez-Garcia SR, Garcia-Gonzalez L, Vorobiev YV, Luna-Barcenas G, Gonzalez-Hernandez J (2002) J Phys Chem B 106:1550
21. Pantelie N, Seliskar CJ (2007) J Phys Chem C 111:18595
22. Shinozaki R, Nakato T (2004) Langmuir 20:7583
23. Shinozaki R, Nakato T (2008) Micropor Mesopor Mater 113:81
24. Ma JJ, Zhang XB, Yan C, Tong ZW, Inoue HR (2008) J Mater Sci 43:5534. doi:10.1007/s10853-008-2837-1
25. Martinez VM, Arbeloa FL, Prieto JB, Arbeloa IL (2005) Chem Mater 17:4134
26. Grauer Z, Avnir D, Yariv S (1984) Can J Chem 62:1889
27. del Monte F, Mackenzie JD, Levy D (2000) Langmuir 16:7377
28. Fujii T, Nishikiori H, Tamura T (1995) Chem Phys Lett 233:424
29. del Monte F, Levy D (1998) J Phys Chem B 102:8036
30. Tani T, Namikawa H, Arai K, Makishima A (1985) J Appl Phys 58:3559